Performance Optimization of a Floating Breakwater Model Using SPH Method, with a Practical Application

D. Alejandro Rueda Duran

Final Report of the Master Thesis

Directed By

Dr. Germán Rodríguez Rodríguez

Dr. Alejandro Jacobo Cabrera Crespo

UNIVERSIDAD DE LAS PALMAS DE GRAN CANARIA

FACULTAD DE CIENCIAS DEL MAR

LAS PALMAS DE GRAN CANARIA

2013

Performance Optimization of a Floating Breakwater Model Using SPH Method with, a Practical Application

Alejandro Rueda[a], Germán Rodríguez[a], A.J.C. Crespo[b]

[a]Departamento de Física, Universidad de Las Palmas de Gran Canaria, 35017 - Las Palmas de Gran Canaria, Spain (grodriguez@dfis.ulpgc.es).
[b]Environmental Physics Laboratory, Universidad de Vigo (Campus de Ourense) - Facultade de Ciencias, As Lagoas, 32004 - Ourense- Spain (alexbexe@uvigo.es).

ABSTRACT

The use of a floating breakwater, as an environmentally friend structure, is suggested as a coastal protection structure for the EGSAM pier in Santa Marta Bay, Caribbean Colombian coast. A large number of floating breakwater structures existing in the literature are examined and compared to define the structure to be used in the studied case. The selection of the more adequate structure is mainly based on two aspects, their dimensions and efficiency, in terms of the wave energy transmission. The efficiency assessment, as a function of the incident wave period and the distance between the floating breakwater and the pier, has been carried out by means of the smoothed particle hydrodynamic (SPH) method, a free-mesh numerical method. Results reveal that SPH method properly simulates the interaction between water waves and a coastal protection structures. Nevertheless, 3D numerical experiments require considerable computational cost, whereas the use of 2D experiments alleviates these drawbacks but include unrealistic effects, mainly due to the presence of closed, non dissipative, boundaries. The proposed structure for the EGSAM pier reveals considerable advantages in contrast with conventional coastal protection structures, which must be evaluated in a wave channel, as part of the design process.

Key Words: Floating Breakwater, Smoothed Particle Hydrodynamic, Waves and Coastal Structures

1. INTRODUCTION

A large number of coastal structures to protect human goods against wind-wave attack, including port facilities both commercial and recreational, have been built during recent decades along the Colombian coasts, especially on the North of the Caribbean coast. However, despite such structures successfully protect coastal zones against waves, mainly due to reasons concerning the preservation of the coastal environment and of aesthetic character, there is an increasing strong negative public reaction to the emplacement of classical rubble-mound breakwaters along the coast. This has led engineers to look for more soft and "environment friendly" coastal protection structures, while ensuring proper safety levels and functionality.

The indiscriminate use of rubble-mound breakwater during the last forty years, as the only alternative to protect small piers, marinas and beaches from erosion, has generated important environmental problems, mainly associated with the interruption or alteration of littoral drift, erosion and pollution. This fact has stimulated interest and research activities for the development of efficient structures helping to preserve the coastal environment. In particular, the use of floating breakwaters (FB hereafter), an old idea (i.e. De la Sala, 1873), has been revisited and picked up as an alternative to protect coastal areas and for generating sheltered areas. The existence of improved facilities to implement more realistic physical models, as well as the development of numerical models and computational capabilities has supported advances in this field.

A clear example of the need to protect a port facility is that of the Santa Marta Coast Guard Station - EGSAM, unit located inside the bay of Santa Marta, which is dedicated to safeguard human life at sea and control illegal activities in the north of the Caribbean coast of Colombia. This pier built in 2005 was designed with the optimum characteristics for mooring, giving service and maintenance of the fast boat assigned to this military unit. However, due to the change in sediment rate of the Manzanares River, which after six seasons of heavy rainfalls has increased its rate of sediment supply and disposal in the zone, leading to a process of accretion under the pier of the EGSAM and inducing a change in the breaking zone position towards the berthing area. As a result, the structure is now partially useless.

The aims of this study is to explore the possibility of improving operating conditions in the EGSAM pier by using a FB, under certain restrictions concerning the fraction of wave energy transmission. For this, numerical experiments, based on the use of the Smoothed Particle Hydrodynamics (SPH) methodology, are performed to simulate monochromatic incident waves and examine the FB efficiency. The final goal is to suggest some efficient FB structure to protect the study case facility.

The remainder of the thesis is structured as follows. Main geographical and climatic conditions of the study area are introduced in section 2. A brief review of the development and main characteristics of FB is presented in section 3. Theoretical basis of the SPH methodology, as well as experimental set-up are described in section 4. Preliminary results derived from numerical simulation concerning wave energy transmission trough the selected floating breakwater geometry are discussed in section 5. Finally, conclusions are summarized in section 6.

2. STUDY AREA

Santa Marta bay is located in the Southwestern side of the Caribbean Sea (11°14’44.98N, 74º13’11.11W), approximately, see Fig. 1.

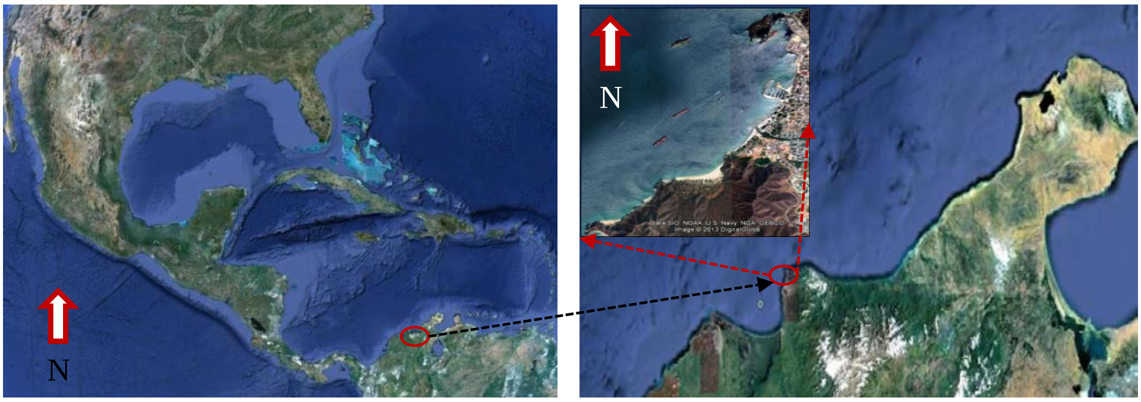

Figure 1. Location map of the Santa Marta bay.

According to the final report of weather conditions for Colombian Caribbean ports, presented by the Center for Hydrographic and Oceanographic Researches (CIOH) in 2010, at a large scale, its weather is influenced by fluctuations in the Azores high pressure system the Inter-tropical Convergence Zone positions. During the dry season (December to April) The Azores high pressure system moves toward lower latitudes leading to an increase in the wind intensity, reaching values over to 3.0 m/s. The predominant direction is determined by the effect of the trade winds, mainly in the dry season, flowing from north and northeast directions during 26% and 15% of the time, respectively (See Table 1). The modal mean wave direction in the zone is from NE, while more severe sea states come from ENE (See

Table 1). Due to fetch restrictions the remainder directional sectors present a very low or null frequency of occurrence.

Data presented in table 1 have been derived from a hindcasting study developed by CIOH for the Colombian Caribbean area covering a period of 32 years, by using the third generation WAM model.

Table 1. Mean wind direction and wave conditions in Santa Marta bay.

Santa Marta Wind Direction	
Direction	**%**
N	26
NE	15
E	4
SE	3
S	10
SO	9
O	8
NO	8
Calm	14

Wave Direction	Significant Wave Height	Wave Period
NE	1.5 - 2.0	5.0 -7.0
ENE	2.0 -2.5	7.0 -9.0
	3.0 -3.5	5.0 -7.1

A recently acquired bathymetry (Colombian Navy Oceanographic and hydrographic Research Center, CIOH, 2012), as well as a recent aerial photo of the study area are shown in Figure 2(a) y 2(b), to facilitate identification of the major geographic features of the zone.

Average temperature is about 28 ° C, and relative humidity is close to 79%. Average rainfall levels are in the order of 98 mm/month, but can change drastically during the rainy season, reaching values close to 330mm/month, in the surroundings to the Sierra Nevada de Santa

Marta, giving rise to a significant increase of the average flow of the rivers in the area, see Figure 3(a-d).

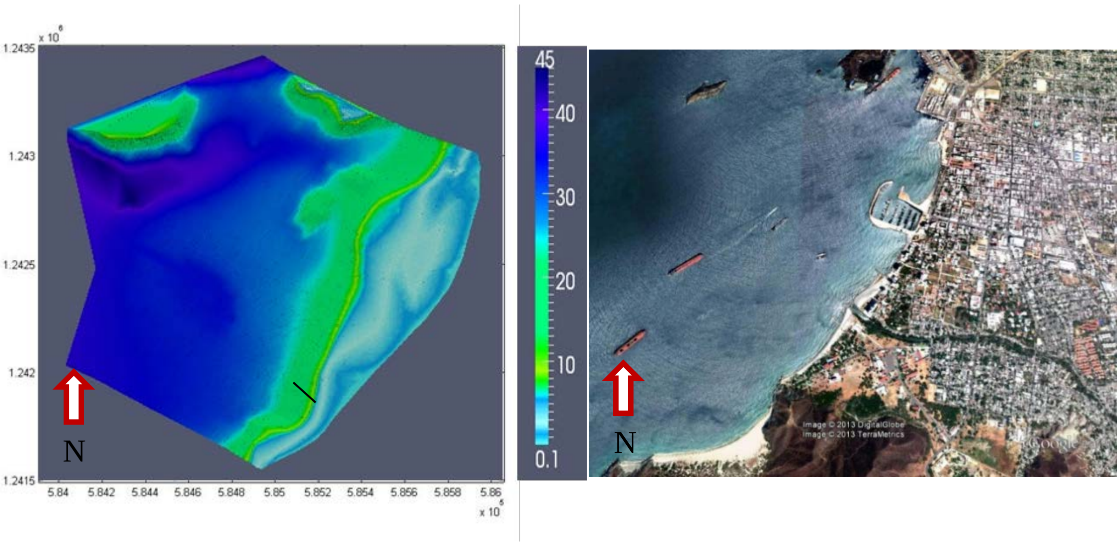

Figure 2. (a) EGSAM Bathymetry (depth in m), (b) Santa Marta Aerial Photo

(a) Year 2006

(b) Year 2009

(c) Year 2011

(d) Year 2012

Figure 3. Effects of Manzanares River sediment rate discharge variability (2006 to 2012).

2.1 FLOATING BREAKWATERS: A SHORT REVIEW

Floating breakwaters (FB) can provide an alternative coastal protection solution with low environmental impact, because its main purpose is to reduce the wave energy transmission to a required level, providing a dynamic equilibrium of the shoreline to preserve existing or artificially nourished beaches, as well as to avoid stagnation zones, by allowing water flow circulation below their bottom tip and the sea bed. A concise definition of floating breakwater was provided by Hales[1]: "*The basic purpose of any Floating breakwater is to protect a part of shoreline, a structure, a harbor, or moored vessels from excessive incident wave energy. Are passive systems; i.e., no energy is produced by the device to achieve wave attenuation. The incident wave energy is reflected, dissipated, transmitted, or subjected to a combination of these mechanisms. The interference of a floating breakwater with shore processes, biological exchange, and with circulation and flushing currents essential for the maintenance of water quality is minimal*".

The efficiency of FB is commonly determined by means of the relationship between the incident wave height (Hi) and the transmitted wave (Ht), known as the transmission coefficient (Kt):

$$Kt = \frac{Ht}{Hi} \tag{1}$$

Assume a FB with rectangular prism (Poonton type) form and considering a two-dimensional view along the wave propagation axis, such as depicted in Figure 4. The water column in the surrounding area can be divided into three sections; (1) a zone before the structure; (2) other just below; and (3) other after the FB. Wave energy approaching to the structure is a function of Hi, while the energy fraction transmitted towards the area to be protected will depend on Ht. Wave energy transmission will also depend, among other factors, on the wavelength, λ, the FB height, Zr, draft, Dr, and width W, as well as of the water depth, h.

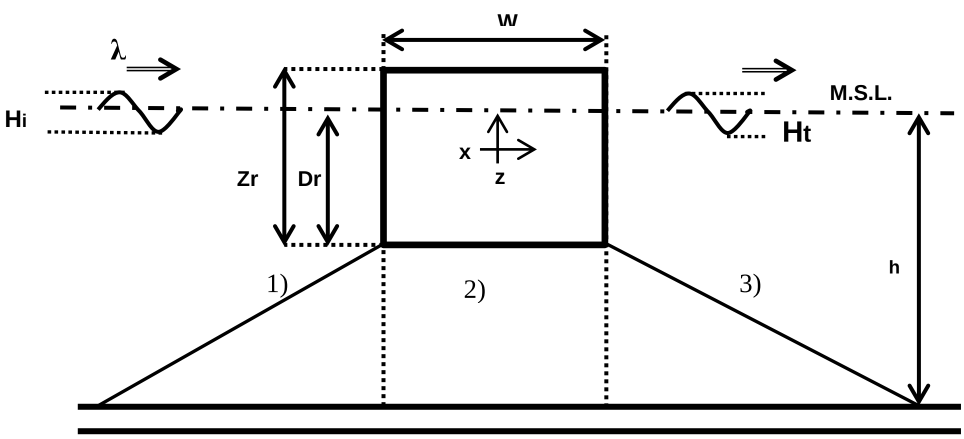

Figure 4. Geometric characteristics of a simple FB.

The use of floating breakwaters as coastal protection structures date back, at least to 1811, when a floating structure was installed to protect the Plymouth Bay (Massachusetts). In that case, a floating breakwater with iron frames of nine feet wide and six feet high, fixed to the bottom with anchors, was used. Used materials were wood and iron, which made its life time very short due to corrosion and biological activity. There are records documenting at least three attempts to use this protection method in the bays of Plymouth and Brighton between 1811 and 1844, De la Sala (1873). The shape of the structures used was very different, but all of them had in common the use of iron frames to contain wooden boxes, and even iron pipes in wooden boxes (see Figure 5), so that the final result was not different to that of their predecessors.

It was not until World War II when the FB use was diversified and began its real optimization from "Phoenix" and "Bombardon" models, developed by the Allies for the

Normandy landing. They also began to be applied as coastal protection barriers, although with very poor results, because having inadequate dimensions, in relation to that of incident waves.

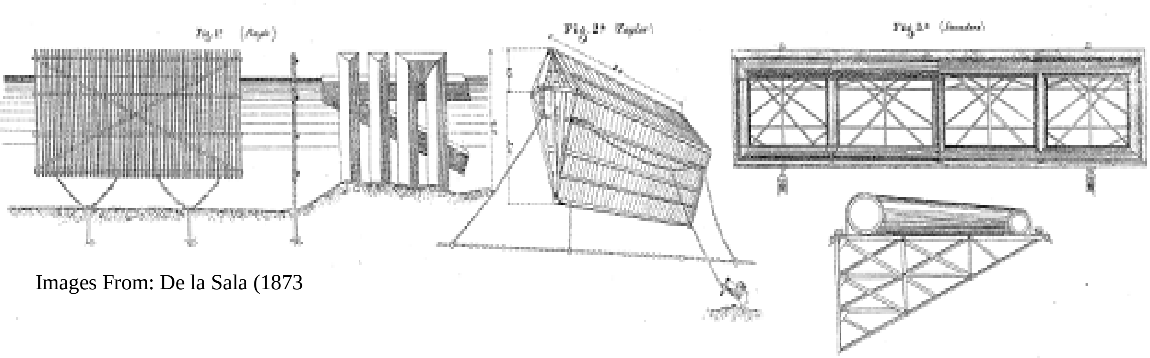

Figure 5. Initial models of floating breakwaters

The most common structural shapes were adequately described in the Coastal Engineering Handbook and are depicted in Figure 6:

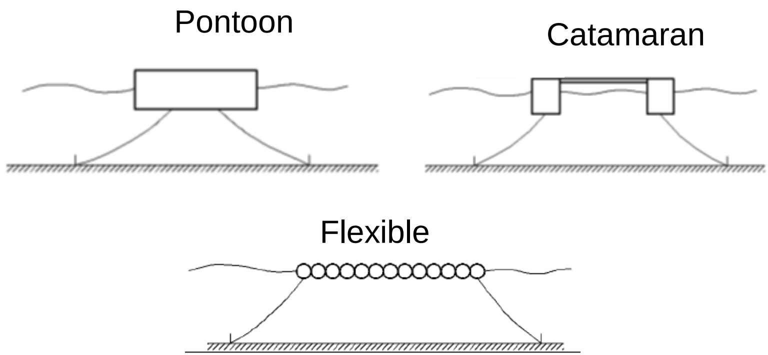

Images From: Coastal Engineering Manual

Figure 6. Most common shapes of floating breakwater

Initially, pontoons were single, evolving towards the use of double structures, the catamaran type, which could be towed from one place to another and reused. Technological evolution made possible the implementation of lighter, filled with polymers for floating, flexible structures (pipelines type), formed by a series of rubber-coated pipes, which can be dismantled and transported to other places.

The theoretical and academic evolution of the FB began, after the Second World War, with the possibility to compare the efficiency of new structures in relation to that used in the Normandy landing, Carr (1950). Some authors like Brebner et al (1958), Wehausen (1971) developed the mathematical description and explanation of the governing equations for a floating body with different degrees of freedom, mainly using the Navier and Stokes equations and demonstrating conservation of mass and momentum, as well as energy conservation, by taking into account that incident energy can be decomposed into reflected, dissipated and transmitted, but without addressing the effect of geometric variations on its hydrodynamic behavior. This fact is considered by Stiassnie (1980) who includes the effect of waves on a simple structure, considering mass and depth of the FB, as well as the characteristics of the tension mooring lines.

In addition to the characterization of FB hydrodynamic behavior, there has been considerable interest on characterizing and grouping the different types of structures designed. Among the various contributions, it is possible to highlight the Coastal Engineering Manual and the reviews by Hales (1981) and Isaacson (1988). Other line of research has focused on the comparison of efficiencies between different shapes, sizes, materials and oceanographic conditions (Volker 1980, Bruce 1985, and Peña 2011). Efficiencies have been examined in terms of transmission, Kt, dissipation, Kd, and reflection, Kr, coefficients, as well as a function of the cost-benefit ratio.

The link between theory and practice is strengthened by the joint implementation of physical and numerical models. The permanent development of computational tools and techniques, as well as improvements in technology used to measure, has allowed increasingly realistic simulations. Physical models were the main simulation tool until the 80s, This approach progressed from simple simulations in wave channels (Brebner 1968, Torun 1987) to experimental validation of 2D models with field measurements in built structures, as shown by Adde (1976) and Yamamoto (1981). In this context, Yamamoto (1981) explored the effect of anchoring lines under effect of the regular and irregular waves, while Bruce (1985) compared the efficiency and cost of various scale and prototype structures With the development experimented during the late 90s by the computational tools, some authors started to make use of numerical modeling, initially under two-dimensional linear wave conditions, to examine FB behavior. It is worth of mention the efforts of some authors by using the Finite Element Method (FEM) to reproduce diffraction and reflection [ie. Isaacson & Sinha (1986), Isaacson & Nwogu (1987)]. With the knowledge improvement provided by using 2D numerical models, other authors developed 3D models to see the deformation to which a structure may be subjected under oblique waves, or the effect in the efficiency by considering the six degrees of movement, Koutandos (2002-2005), Loukogeorgaki (2012). In addition to the use of the most known numerical methods such as FEM, Finite Difference or Finite Fluid Volume, during the last years some few authors has used a free surface method, the Smoothed Particle Hydrodynamic method, for improving the free surface characterization during the simulation process, Shao (2005) and Najafi (2011).

FB is commonly used to protect marine structures, marinas and harbors from wave attacks, however recent advances in this field have stimulated their use in many other fields, such us:

- coastal and shore line protection,
- renewable energy production,
- aquaculture,
- leisure –tourism
- design facilities from aquatic sports.

In general, floating breakwaters can be used under a considerable number of geomorphological and oceanographic conditions. Bruce (1985) enumerates the following principal advantages:

- FB may be the only solution where poor foundations will not support bottom-connected breakwaters.
- FB installations are less expensive than rubble-mound breakwaters.
- FB presents a minimum of interference with water circulation.
- FB is easily moved and can usually be rearranged into new layout with minimum effort.
- FB has a low profile and presents a minimum intrusion on the horizon, particularly for areas with high tide ranges.

However, it is worth noting that floating breakwaters in general, may have serious disadvantages. The most significant are, Hales (1981):

- The design of a floating breakwater system must be carefully matched to the site conditions (bottom changes, wind fetch, etc.) with due regard to the longer waves which may arrive from infrequent storms.

- The floating breakwater can fail to meet its design objectives by transmitting a larger wave than can be tolerated without necessarily suffering structural damage.
- A major disadvantage is that floating breakwaters move in response to wave action and thus are more prone to structural-fatigue problems.

3. METHODOLOGY

To reproduce the weather conditions from Santa Marta, the characteristics (shape and dimensions) by EGSAM pier and FB to use, we employed a numerical method called Smoothed Particle Hydrodynamics (SPH) which reproduces the domain, the fluid and the objects with which it interacts from of particles which have characteristics of position, velocity, mass and density.

3.1 Smoothed Particle Hydrodynamics

SPH is a Lagrangian method developed 30 years ago (Lucy, 1977; Gingold and Monaghan, 1977; Monaghan, 2005) in astrophysics and cosmology. In recent years this method has been applied to study of free surface hydrodynamics problems.

SPH is a mesh free method that eliminates restrictions resulting from the use of Eulerian methods, which discretizes the physical medium making use of a mesh that covers it completely, so that the places where there are interactions and the empty spaces are treated equally. This causes an increase in the calculation time and inefficient use of memory system. However, Lagrangian methods do not use a mesh to define the computational domain, the volume to be considered is that in which fluid particles are present, empty areas are not considered, and therefore the memory resources are optimized. In SPH the fluid domain is decomposed into a set of irregularly spaced nodal points, called particles where physical properties (e.g., mass, density, velocity, position, pressure) are known, and which interact with each other according to the fluid conservation laws.

SPH uses a kernel function to make possible the transition from a continuous (fluid) to a discrete medium (particles). This function has a compact support within a region determined by a distance much smaller than the characteristic scale of the problem. This distance, defined by the kernel, is the distance of particle interaction and determines the model accuracy.

The SPH code employed in this study, DualSPHysics, is a joint effort by researchers at the University of Vigo (Spain), the University of Manchester (UK) and the Johns Hopkins University (U.S.A.). This code has been mainly applied to the study of coastal processes 2D (Gómez-Gesteira et al., 2005; Dalrymple y Rogers, 2006; Crespo et al., 2008) and 3D (Gómez-Gesteira y Dalrymple, 2004; Crespo et al., 2007a). DualSPHysics is a free code that is freely available at (www.sphysics.org).

In SPH, the fundamental principle is to approximate any function *A(**r**)* by:

$$A(\mathbf{r}) = \int_{\Omega} A(\mathbf{r}')W(\mathbf{r}-\mathbf{r}',h)d\mathbf{r}' \tag{2}$$

where ***r*** is the particle position; *W* is the weighting function or kernel; *h* is the weighting function smoothing length controls the domain Ω (see Figure 7). The parameter *h*, often called influence domain or smoothing domain, controls the size of the area around particle a where contribution from the rest of the particles cannot be neglected.

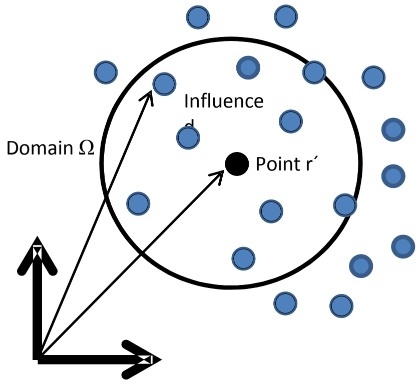

Figure 7. Sketch of the influence domain of a particle.

The approximation (2), in discrete notation, leads to the following approximation of the function at the particle (interpolation point) a:

$$A_a = \sum_b m_b \frac{A_b}{\rho_b} W_{ab} \tag{3}$$

where the summation is overall the particles (b) within the region of compact support of the kernel function, fixed by h. The mass and density are denoted by m_b and ρ_b respectively and $W_{ab} = W(r_a - r_b, h)$ is the weighting function or kernel between two particles a and b.

- *Kernel function*

The performance of SPH models depends on the choice of the weighting function, which should satisfy several conditions such as:

- Positivity: $W(r_a - r_b, h) \geq 0$ in the domain Ω
- Compact support: $W(r_a - r_b, h) = 0$ out the domain Ω
- Normalization: $\int_\Omega W(\mathbf{r_a} - \mathbf{r}_b, h) d\mathbf{r}_b = 1$
- Delta function behavior: $\lim_{h\to 0} W(\mathbf{r_a} - \mathbf{r}_b, h) d\mathbf{r}_b = \delta(\mathbf{r_a} - \mathbf{r}_b)$
- Also W_{ab} must be monotonically decreasing within creasing distance from particle a.

Kernels depend on the smoothing length, *h*, and the non-dimensional distance between particles given by $q = {r_{ab}}/{h}$ where r_{ab} is the distance between particles a and b $\left(r_{ab=r_a-r_b}\right)$.

The Lagrangian form of the Navier-Stokes set equation is written as follows:

- *Momentum equation*

The momentum conservation equation in a continuum field is:

$$\frac{D_v}{Dt} = -\frac{1}{\rho}\boldsymbol{\nabla}P + \mathbf{g} + \boldsymbol{\Theta} \tag{4}$$

where **v** is the velocity, *P* y *ρ* are pressure and density, **g** = (0,0,-9.81)ms^{-2} is the gravitational acceleration and $\boldsymbol{\Theta}$ refers to the diffusion terms.

The pressure term is expressed in SPH notation as:

$$-\frac{1}{\rho}\boldsymbol{\nabla}P = -\sum_b m_b\left(\frac{P_a}{\rho_a^2} + \frac{P_b}{\rho_b^2}\right)\boldsymbol{\nabla}_a W_{ab} \tag{5}$$

where P_b y ρ_b are pressure and density corresponding to a particle a and b and $W_{ab} = W(r_a - r_b, h)$ is the *kernel* function.

Then, the SPH momentum equation, Monaghan (1992) becomes:

$$\frac{d\mathbf{v}_{\boldsymbol{a}}}{dt} = -\sum_b m_b\left(\frac{P_a}{\rho_a^2} + \frac{P_b}{\rho_b^2}\right)\boldsymbol{\nabla}_a W_{ab} + \mathbf{g} \tag{6}$$

Different approaches, based on various existing formulations of the diffusive terms, can be considered in the SPH method to describe the momentum equation.

- *Viscosity*

Two different options for diffusion can be used in SPH: artificial or laminar viscosity.

- Artificial Viscosity

The artificial viscosity proposed by Monaghan (1992) has been used very often due to its simplicity. In SPH notation Eq. (6) can be written as:

$$\frac{d\mathbf{v}_a}{dt} = -\sum_b m_b \left(\frac{P_a}{\rho_a^2} + \frac{P_b}{\rho_b^2} + \Pi_{ab}\right) \boldsymbol{\nabla}_a W_{ab} + \mathbf{g} \tag{7}$$

where Π_{ab} is the viscosity term:

$$\Pi_{ab} = \begin{cases} \dfrac{-\alpha\overline{c_{ab}}\mu_{ab}}{\overline{\rho_{ab}}}, & if\ \mathbf{v}_{ab}\cdot\mathbf{r}_{ab} < 0 \\ 0, & otherwise \end{cases} \tag{8}$$

with

$$\mu_{ab} = \frac{h\mathbf{v}_{ab}\cdot\mathbf{r}_{ab}}{\mathbf{r}_{ab}^2+\eta^2} \tag{9}$$

where $\overline{\rho_{ab}} = \frac{1}{2}(\rho_a+\rho_b)$, $\overline{c_{ab}} = \frac{1}{2}(c_a+c_b)$; $\eta^2 = 0.01h^2$; α is a free parameter that can be changed according to each problem.

- Laminar Viscosity

The momentum conservation equation with laminar viscous stresses is given by:

$$\frac{D\mathbf{v}}{Dt} = -\frac{1}{\rho}\boldsymbol{\nabla}P + \mathbf{g} + \upsilon_0\nabla^2\mathbf{v} \tag{10}$$

where the laminar stress term simplifies Morris et al., (1997), Lo and Shao (2002) to:

$$(\nu_0\nabla^2\mathbf{v})_a = \sum_b m_b\left(\frac{4\nu_0\mathbf{r}_{ab}\boldsymbol{\nabla}_a W_{ab}}{(\rho_a+\rho_b)|\mathbf{r}_{ab}|^2}\right)\mathbf{v}_{ab} \tag{11}$$

where ν_0 is the kinetic viscosity of laminar flow ($0.893\cdot10^{-6}$ m^2/s). So, in SPH notation, Eq. (11) can be written as:

$$\frac{d\mathbf{v}_a}{dt} = -\sum_b m_b\left(\frac{P_a}{\rho_a^2}+\frac{P_b}{\rho_b^2}\right)\boldsymbol{\nabla}_a W_{ab} + +\mathbf{g} + \sum_b m_b\left(\frac{4\nu_0\mathbf{r}_{ab}\boldsymbol{\nabla}_a W_{ab}}{(\rho_a+\rho_b)|\mathbf{r}_{ab}|^2}\right)\mathbf{v}_{ab} \tag{12}$$

- *Continuity Equation*

Changes in the fluid density are calculated in DualSPHysics using:

$$\frac{d\rho_a}{dt} = \sum_b m_b\mathbf{v}_{ab}\boldsymbol{\nabla}_a W_{ab} \tag{13}$$

instead of using a weighted summation of mass terms (Monaghan, 1992), since it is known to result in an artificial density decrease near fluid interfaces.

- *Equation of State*

The fluid in the SPH formalism can be treated as weakly compressible. This facilitates the use of an equation of state to determine fluid pressure, which is much faster than solving an equation such as the Poisson´s equation. Following (Monaghan et al., 1999; Batchelor, 1974), the relationship between pressure and density is assumed to follow the expression:

$$P = B\left[\left(\frac{\rho}{\rho_0}\right)^{\gamma} - 1\right] \tag{14}$$

where B is a constant related to the modulus of compressibility of the fluid, $\rho_0 = 1000.0\ {}^{Kg}/_{m^3}$ being the reference density, usually at the free surface and γ is a constant between 1 and 7 (although 7 is used in most of the oceanic applications).

The speed of sound *c*, depends on the derivative of pressure with respect to density:

$$c^2(\rho) = \frac{\partial P}{\partial \rho} = \frac{B\gamma}{\rho_0}\left(\frac{\rho}{\rho_0}\right)^{\gamma-1} = \frac{B\gamma}{\rho_0^{\gamma}}\rho^{\gamma-1} \tag{15}$$

$$c_0^2 = c^2(\rho_0) = \frac{\partial P}{\partial \rho}\Big|_{\rho=\rho_0} = \frac{B\gamma}{\rho_0} \tag{16}$$

where c_0 is the speed of sound at the reference density; $B = c_0^2\rho_0/\gamma$. Additionally, B provides a limit for the maximum allowed change of density in each simulation.

3.2 Box Model Design and code validation

The problem to study presents a 3D nature. However, to reduce the computational time, several experiments were carried out in a 2D domain. The main goal of these 2D simulations has been to assess the usefulness and possible limitations of the methodology to explore the problem under study, especially in terms of the bathymetry. After these, the final steps of the study have been developed by using a 3D domain. The following dimensions have been used for the box model design: 300m long, 100m wide (3D) and 45m depth (see Figure 8). The wavemaker in the numerical tank is a piston-type wave generator. Separation between particles has been established as 0.25m. The number of particles used in the 2D model is 121.812 and 7.264.747 in 3D experiments.

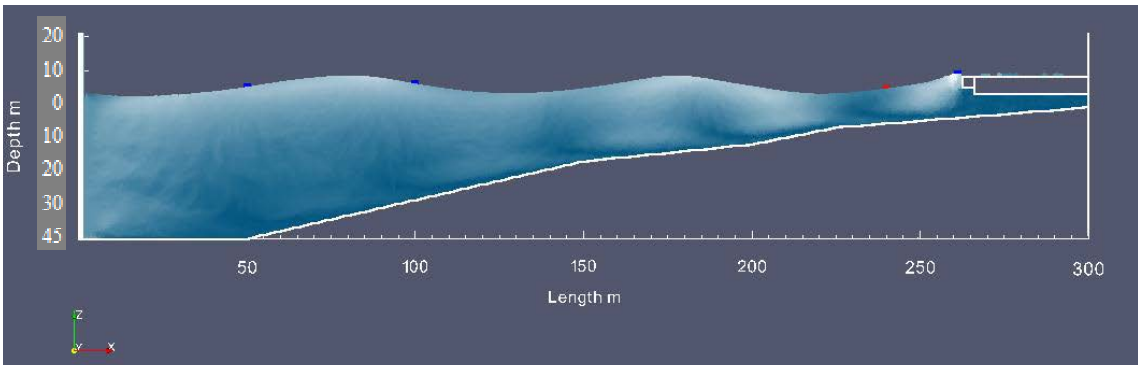

Figure 8. Configuration of the 2D numerical tank.

It is important to remark the hypothesis underlying the experiments: (a) the FB has a position which is fixed in space, so that the possibility of energy radiation is eliminated, and (b) the FB is infinitely long in alongshore direction in 2D, (c) due to shoaling effects, the wave propagation direction is almost perpendicular to the beach. Hence, all simulations were carried out with the FB located parallel to pier line, d) the structures were designed using a reference depth of $h = 20$m and a period $T = 7$s. Furthermore ideal and weakly compressible fluid and irrotacional flow are assumed, as well as the applicability of lineal wave theory.

The FB structure used to validate the applicability of the methodology to tackle the proposed study, has been that proposed by Bruce (1985). A total of 90 simulations were carried out in

2D with the aid of two Graphic Processing Units (GPU) with the support from the Environmental Physics Laboratory of the University of Vigo.

The first problem evidenced while carrying out 2D experiment has been the large importance acquired by wave reflection, since in this case the box model behaves like a closed box. Progressive input of wave energy to the numerical wave tank and successive reflections will give rise to harbor agitation problems which, for some incident wave periods can give rise to resonance conditions. Naturally, these phenomena are frequent in the nature when wave energy propagates into or towards a closed or semi-enclosed basing. However, in the present simulations, these are mainly an artifact generated by using a 2D box model. Note that in a 2D model, the lateral boundaries, especially those constituted by the wavemaker and the pier fully close the domain of study, such that energy cannot be properly dissipated, as occurs in the beach placed behind the pier in nature (Fig. 1).

The validation procedure consisted of six different simulation experiments: a) without bathymetry, b) bathymetry with constant slope of 9%, c) bathymetry with constant slope of 18%, d) a bathymetry designed to strokes, e) Santa Marta's actual bathymetry and, f) bathymetry with constant slope of 16%, without pier, X = 350m and a 50m length beach. The latter case was considered to enhance wave energy dissipation, reducing reflection effects. Points to measure wave height have been placed at 1.5, 25, 165 and 200m separated from the pier. The values wave heights were numerical measured by using post-processing tools of the DualSPHysics code.

Each experiment has been performed for 160s of physical time. Since average wave period in Santa Marta is around T = 7s, simulations were performed for periods T = 6, 7 and 8 s. The FB efficiency was evaluated at four different distances (50, 75, 100 and 150 m) from the EGSAM pier. The existence of harbor oscillations induced by incident and reflected waves in simple geometries can be predicted by means of the Merian formula (ie., Sorensen, 1993), which in two-dimensional conditions is given by:

$$T_n = \frac{2L}{n\sqrt{gh}} \tag{16}$$

where T_n is the natural period of oscillation, L is the length of the domain, n the number of nodes, g the gravitational acceleration and h the basin depth. Furthermore, the critical ratio of resonance occurrence between the wavelength λ and the domain length L, in enclosed and semi-enclosed basins are given in Table 2 (Sorensen, 1993).

Table 2. Critical values of λ/L inducing resonance conditions.

Open-ended Basin Critical Periods	**0.25**	**0.75**	**1.25**	**1.75**	**2.25**
Closed Basin Critical Periods	**0.5**	**1**	**1.5**	**2**	**2.5**

To compare theoretical reflection and transmission coefficient with the values observed in the numerical wave tank, the following equations can be derived:

$$\frac{H_R}{H_i} = \left[\frac{E_R}{E_I}\right]^{1/2} = \left[1 - \frac{\sinh[4*\pi\,(h-Dr)/\lambda]}{\sinh 4\pi h/\lambda}\right]^{1/2} \tag{17}$$

$$\frac{H_t}{H_i} = \left[{H_i}^2 - {H_R}^2\right]^{1/2} = \left[\frac{\sinh[4*\pi\,(h-Dr)/L]}{\sinh 4\pi h/L}\right]^{1/2} \tag{18}$$

where, E_R y E_i are the reflected and transmitted energy, respectively.

3.3 Floating Breakwaters Assessment

The selection of the FB structure to be evaluated has been done after an in-depth literature review. Fourteen cases, including structural information of the FB and properly described wave conditions in physical, numerical or actual cases, were considered for further analysis, by taking into account the usefulness of the information provided (see Table 3).

The numerical implementation of the FB structures in the model has been developed by using dimensionless relationships between geometrical dimensions of the structure, bathymetry and wave parameters given in Table 3. This methodology makes possible comparisons between structures with different dimensions. The efficiency of each one of the selected structures has been assessed by using the average wave and bathymetric conditions recorded in Santa Marta Bay.

The efficiency of these fourteen selected structures was compared using a decision matrix in which the transmission coefficient $K_t$and volume of the structure are evaluated to select that offering a better balance between efficiency and geometrical dimensions, or cost.

Table 3. FB Methodology Design

References	Thesis Code	Place	Height FB /Draft Zr/Dr	Wide / Draft W/Dr	Wave Height/ Depth H/h	Depth/ Wave Lenght h/λ	Wide/ Wave Lenght W/λ	Draft / Depth Dr/h	Wave Height/ Wave Lenght Hi/λ	Dimentional Depth 2πh/λ
Brebner (1968)	Case 1	Physical Model	2,221844	7,5647092	0,200	0,345	0,383	0,147	0,069	2,167
Bruce (1985)	Case 2	Olympia Harbor (Washington)	1,5714286	6	0,156	0,196	0,165	0,140	0,031	1,231
Torum (1987)	Case 3	Physical Model	1,4285714	4,6869141	0,123	0,223	0,091	0,088	0,027	1,401
Manuel (1995)	Case 4	Physical Model	1,3333333	2	0,032	0,620	0,248	0,200	0,020	3,895
Murali (1997)	Case 5	Physical Model	1,4347826	2,826087	0,200	0,108	0,141	0,460	0,022	0,680
Sannasiraj (1998)	Case 6	Physical and Numerical Model	4	4	0,019	0,510	0,087	0,043	0,010	3,203
Allyn (2004)	Case 7	Physical Model	1,2352941	2,2941176	0,076	0,326	0,127	0,170	0,025	2,046
Fouster (2007)	Case 8	Numerical Model	1,25	2,25	0,123	0,396	0,178	0,200	0,049	2,488
Martinelli (2008)	Case 9	Physical Model	2,3333333	6,6666667	0,170	0,246	0,105	0,064	0,042	1,545
Elchahal (2009)	Case 10	Numerical Model	1,1315789	0,6644737	0,050	0,401	0,101	0,380	0,020	2,518
Wang (2010)	Case 11	Numerical Model	1,1111111	1,6	0,150	0,168	0,135	0,450	0,025	0,731
Yoon (2011)	Case 12	Physical and Numerical Model	2,6666667	6,6666667	0,086	0,116	0,106	0,136	0,010	0,731
He (2012)	Case 13	Physical Model	2,259887	8,7570621	0,044	0,225	0,388	0,197	0,010	1,414
Loukogeorgaki (2012)	Case 14	Numerical Model	1,8181818	4,5454545	0,037	0,158	0,250	0,347	0,006	0,995

The three more efficient structures, in terms of wave energy reduction and dimensions, were considered to decide the geometrical shape of the FB to be suggested as an initial optimal infrastructure for the study area, both in 2D and 3D. For this, 75 numerical experiments were carried out in 2D.

4. RESULTS AND DISCUSSION

A first observed result is that in 2D simulations the wave reflection from the front and backside boundaries plays a dominant role, due to the lack of energy dissipating areas. Furthermore, it has been observed that wave conditions become stable after some transient period. Thus, only a final part of the total wave data record measured has been considered to examine the resulting conditions associated to each case. (See figure 9).

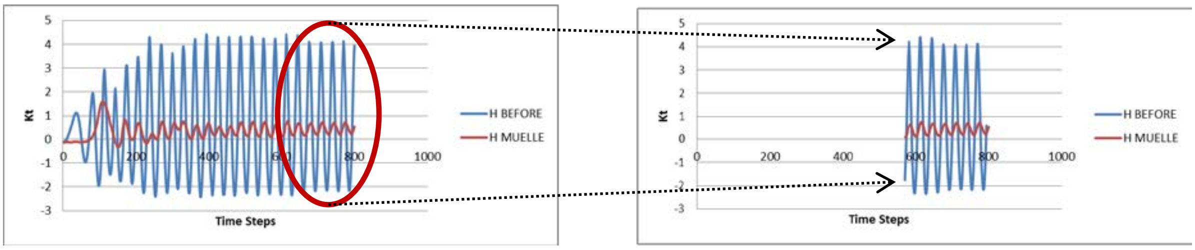

Figure 9. Fraction of wave data series selected to be analyzed.

When a wave train propagates towards beach and meets the FB, part of the incident energy is reflected. Another part of the fraction transmitted through the structure can be reflected at the sloped bottom, at the deck, and at the front boundary of the box model. In this sense, for all the studied cases, when the FB was placed at a distance of 50, 75 and 100m from the pier, the box model behaved like a semi-enclosed basin, with the reflection between FB and the pier been the most important effect. When the FB was located 150m apart from the pier, in the middle of the box model domain, the reflection effect was the same both between the piston and the structure, as between the pier and the FB, so that in this condition the box model behaves in a similar way to a closed basin.

All the simulations have revealed that wave energy transmission increases with the period of the incident waves. In other words, efficiency of FB decreases with the length of the incident waves.

In the first simulation, carried out without bathymetry (see Figure 10a) it has been found that basin oscillations are considerable when the structure is separated 75m from the pier, for periods of 8 and 6 s, inducing oscillating modes close to T_3 and T_1, respectively. When the wave period is 7s, this phenomenon was mainly observed with the FB structure placed at 100 and 150m far from the deck.

Adding a bottom slope of 9%, simulations of Figure 10b reveal that for shorter wave period, 6s, the effect of basin oscillation reduces because of this phenomenon is particularly relevant to long waves, and is intensified for longer periods. This enhancement is particularly notable for T=8s, due to the match with the critical period given by the Merian expression, (Sorensen 1993).

By increasing the slope (see Figure 11a), it is observed that the transmission coefficient moderately reduces. This is probably due to the increase in wave energy dissipation by bottom friction. However, the general behavior remains similar and continues along validation test by using 2D numerical tank.

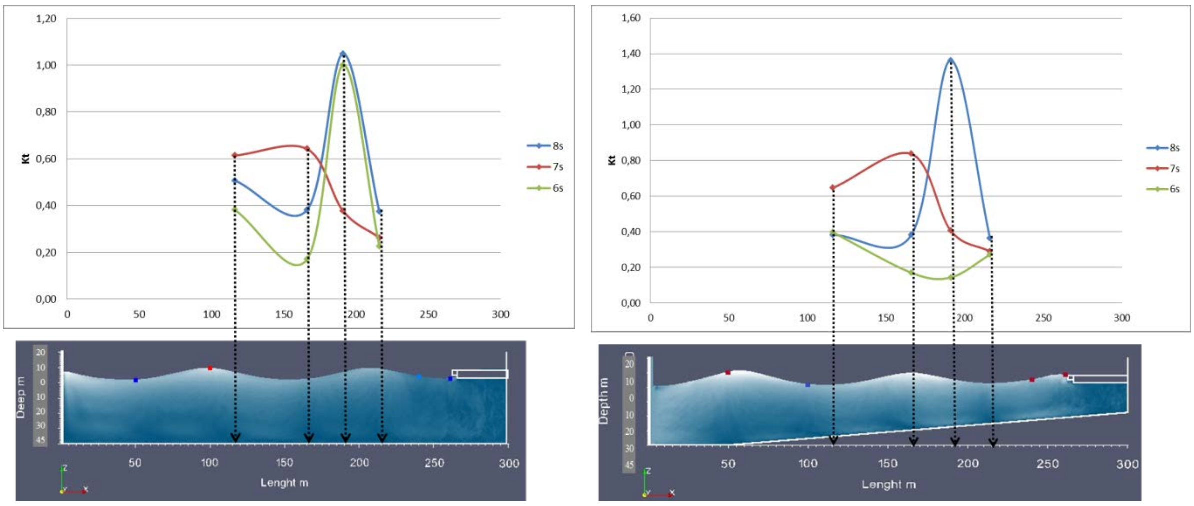

Figure 10. Case study with (a) flat bottom, (b) with 9% slope

For the uneven bathymetry (see Figure 11b), smoothly adapted to the actual bathymetry of Santa Marta Bay, the energy dissipation enhances and the coefficient of transmission tends to present a behavior closer to that theoretically expected. Nevertheless, longer periods still induce important oscillations in the basin, but for any distance between the FB and the pier Kt decreases with the wave period, as expected.

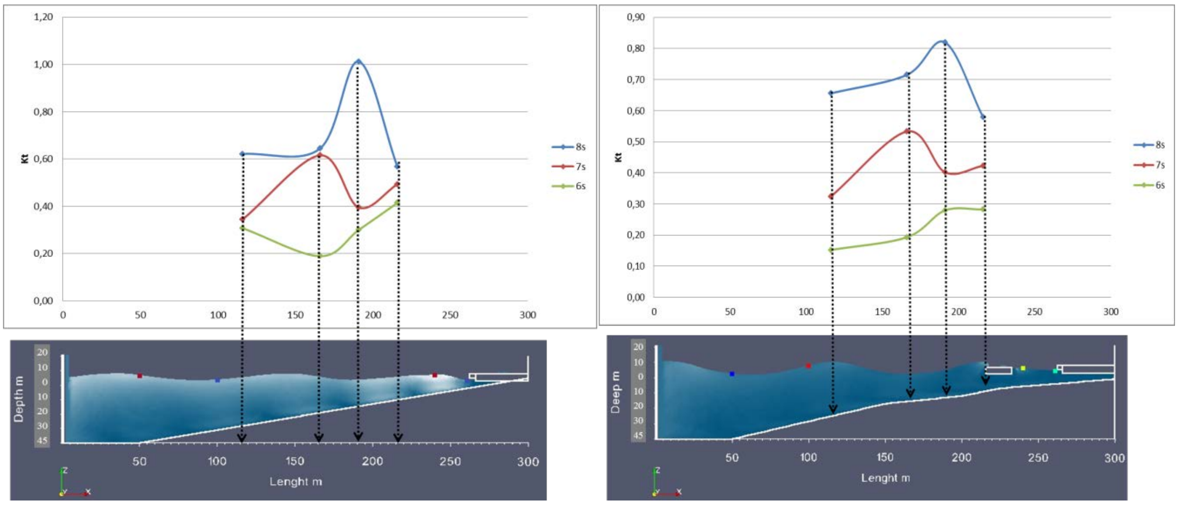

Figure 11. Case study with (a) 18 % slope and (b) with smooth out bathymetry

Removing the restriction imposed by the presence of the pier in the front boundary of the box model but including a linear slope that extends backwards, acting as a beach (Fig. 12a), a drastic reduction in the fraction of energy reflected can be observed and, as consequence, the basin oscillation reduces and Kt suffers a reduction close to 50-70%. Thus, standing waves generated in the model are mainly due to reflection in the pier boundary, which is unrealistic. Reflection from the bottom slope can occur in nature, but is considerably less important. Other problem difficult to solve in the 2D case is the reflection experimented by waves returning to the wavemaker.

By comparing the behavior of the transmission coefficients obtained in the previous case with that observed in the 2D experiment carried out by using a transect of the actual bathymetry of Santa Marta (Fig. 12b), a clear similarity in the FB behavior efficiency is observed for any wave period and relative FB location.

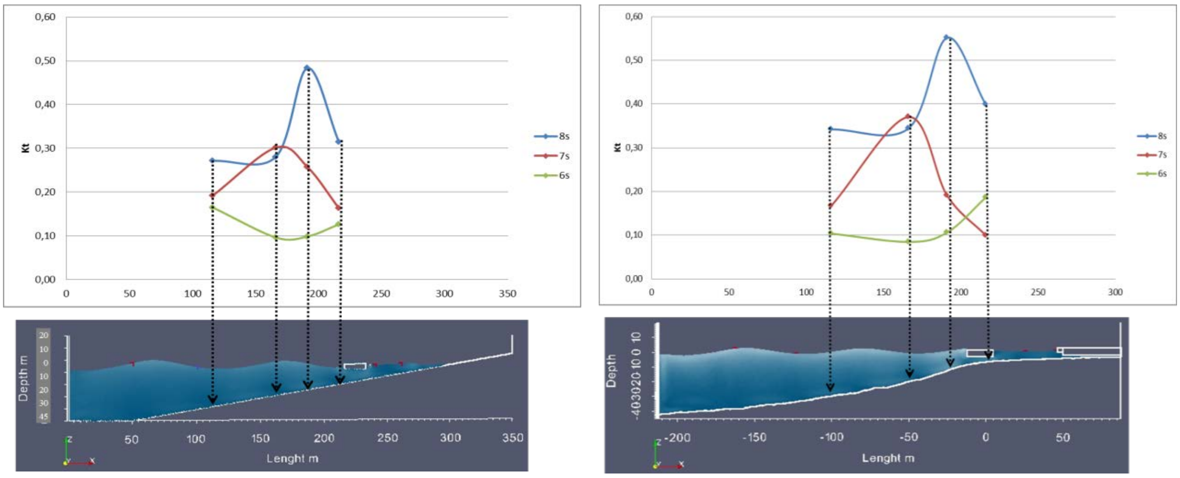

Figure 12. Case study (a) without deck (b) real bathymetry in Santa Marta

Above exposed results highlight that under these conditions the simplified 2D model allows to explore the comparative efficiency of several FB designs by reducing extraordinarily the computation time, though some observed phenomena are not physically realistic.

Accordingly and taking into account the dimensionless parameters given in Table 4, fourteen structures have been designed (see Table 4) and their efficiencies examined by considering a reference depth h = 20m and a wave period T = 7s.

Table 4. Dimensions of the 14 FB tested.

PARAMER/CASE	1	2	3	4	5	6	7	8	9	10	11	12	13	14
Z_R	6,55	4,4	2,5	5,33	13,2	3,4	4,2	5	2,97	8,6	10	7,27	8,88	12,63
X_R	22	16,8	8,2	8	26	3,4	7,8	9	8,51	5,05	14,4	18,18	34,4	31,57
Dr	2,93	2,8	1,75	4	9,2	0,85	3,4	4	1,27	7,6	9	2,72	3,93	6,94
ERROR	(+/-) 0,25	(+/-) 0,25	(+/-) 0,25	(+/-) 0,25	(+/-) 0,25	(+/-) 0,25	(+/-) 0,25	(+/-) 0,25	(+/-) 0,25	(+/-) 0,25	(+/-) 0,25	(+/-) 0,25	(+/-) 0,25	(+/-) 0,25
Area FB m2	**144,1**	**73,92**	**20,5**	**42,64**	**343,2**	**11,56**	**32,76**	**45**	**25,27**	**43,43**	**144**	**132,2**	**305,5**	**398,7**

Comparison of the 14 FB in terms of structural dimensions (2D) and energy transmission reduction (See Fig.13), permitted to classify the structures into three groups. The first group includes the cases 1, 11, 12, 12 and 14. The second group is formed by cases 2, 4, 5, 7, 8 and 10, while the third group contains the cases 3, 6 and 9.

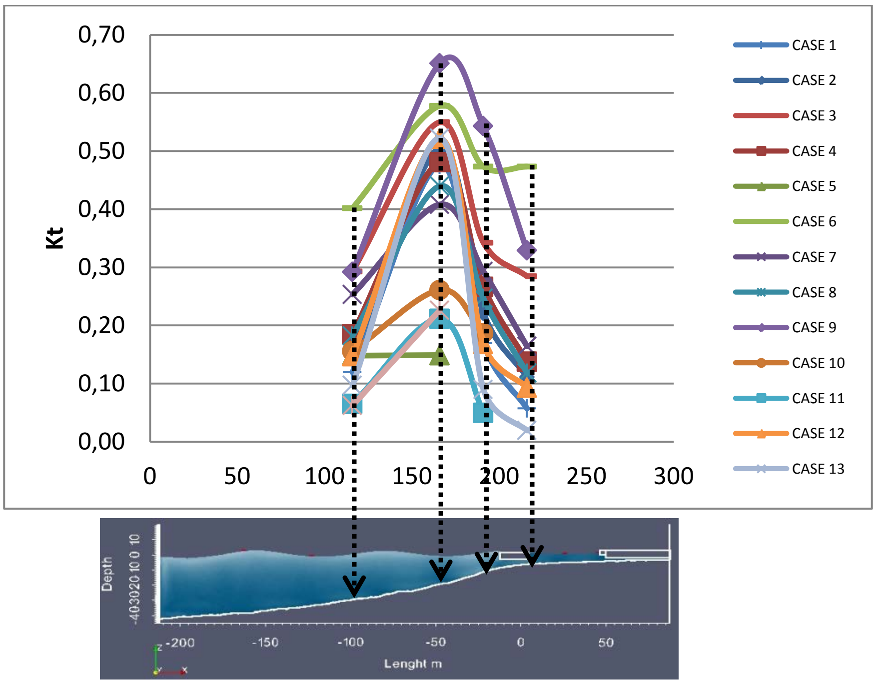

Figure 13. Efficiency comparison from the 14 cases of study.

Note that, due to the dimensions associated to the cases 5 and 1, these cannot be placed at the 50m position. The same occurs for cases 11 and 14 at 50 and 75m locations.

Comparison of theoretical and experimental values for transmitted and reflected energy makes evident that for the average of the fourteen cases, the experimental values are substantially lower than those predicted (see Table 5). Explanation resides mainly in the fact that theoretical estimations do not include energy dissipation, while the model takes into account fluid friction with bottom and with the floating structure.

Table 5. Theoretical and experimental (SPH-2D) Hi and Ht.

Parameters	**FB Distance to Pier**			
	50m	**75m**	**100m**	**150m**
Hi	4,81	3,43	1,75	4,11
Ht Theoric	2,69	2,21	1,24	2,95
Ht SPH	0,73	1,06	1,07	0,93
h	7	7	7	7
Dr	4	4	4	4
λ	55,11	62,89	73,69	75,85
T	7	7	7	7

Using a decision matrix (see Table 6) the three more efficient FB, cases No. 3, 4 and 11, were selected. The highest value (1.0) is assigned to the lowest Kt and (1.0) to the smaller area.

Table 6. Decision matrix used to selected the most efficient cases

Set 1	**FB Vol.**	**Kt**	Overall
1	0,60	0,40	1,00
11	0,8	0,8	1,60
12	1,00	0,4	1,40
13	0,40	1,00	1,40
14	0,2	0,60	0,80

Set 2	**FB Vol.**	**Kt**	Overall
2	0,33	1,00	1,33
4	0,83	0,66	1,49
5	0,16	0,5	0,66
7	1,00	0,33	1,33
8	0,50	0,83	1,33
10	0,66	0,33	0,99

Set 3	**FB Vol.**	**Kt**	Overall
3	0,66	1,00	1,66
6	1,00	0,33	1,33
9	0,33	0,66	0,99

The most efficient dimensions have been considered to develop the final FB to be proposed for Santa Marta (Case 15): Z_R= 6.5m, X_R= 6.0m and D_R= 4.0m, with an area of $39m^2$ (2D) and a volume of ($1560m^3$ −3D). After comparing the cases 1, 3, 4 and 15 (See Figure 13) it is observed that, despite having a substantially smaller area, its efficiency remains within an adequate ranges.

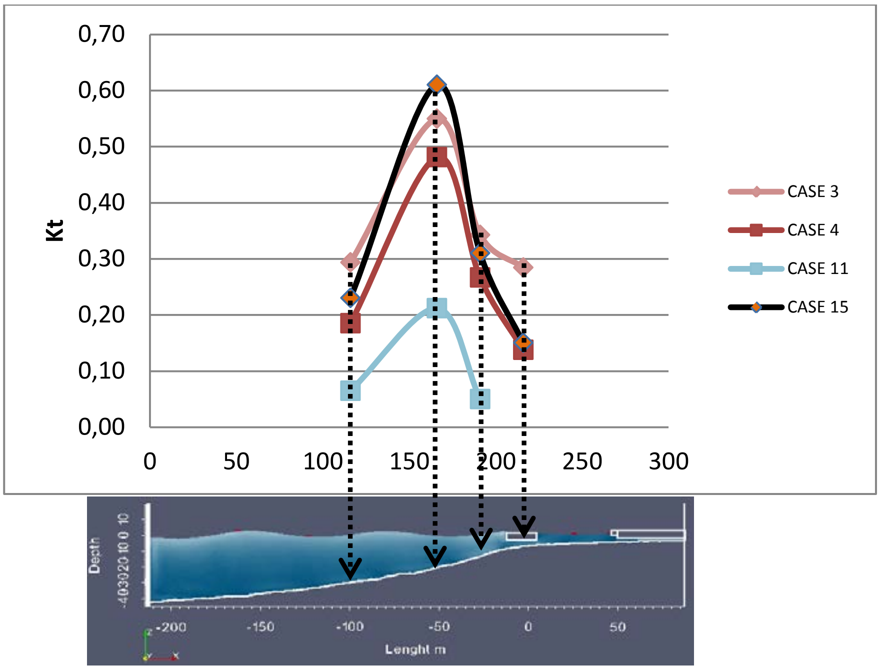

Figure 13. Comparison of the most efficient cases vs. the proposed case.

Once defined the structure to be proposed to protect the EGSAM pier, more realistic and robust experiments by considering the actual topography of the study area have been conducted in 3D simulation of the most efficient condition (FB located at 50m from pier) for a period T = 7s.

It has been found that the 3D model (Figure 14) accurately reproduces:

- The diffraction effects on the sides of the FB.
- The reflection effect throughout the pier and the FB.
- The energy dissipation by shoaling effect in the back zone to the pier.
- The wave set was stabilized at 50 time steps vs. the 350 requiring in 2D.

In general 3D model reproduce the real conditions (reducing resonance and reflection), the wave incident wave height decrees 45% and a transmitted wave 60%, which is directly reflected in the transmission coefficient values, having a reduction of 50% (see Figure 15).

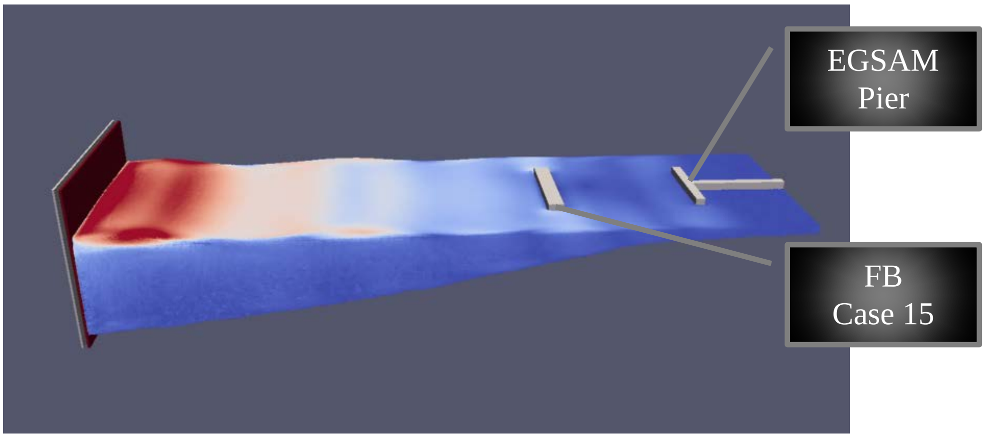

Figure 14. Case 15 - 3D FB, proposed for Santa Marta.

It is important to note that having the domain 80m wide and the FB wide=40m, the diffraction effect is confined to 20m on either side of the structure and that not having a beach in the pier back zone, remains minimal non real reflection by the interaction with the contour.

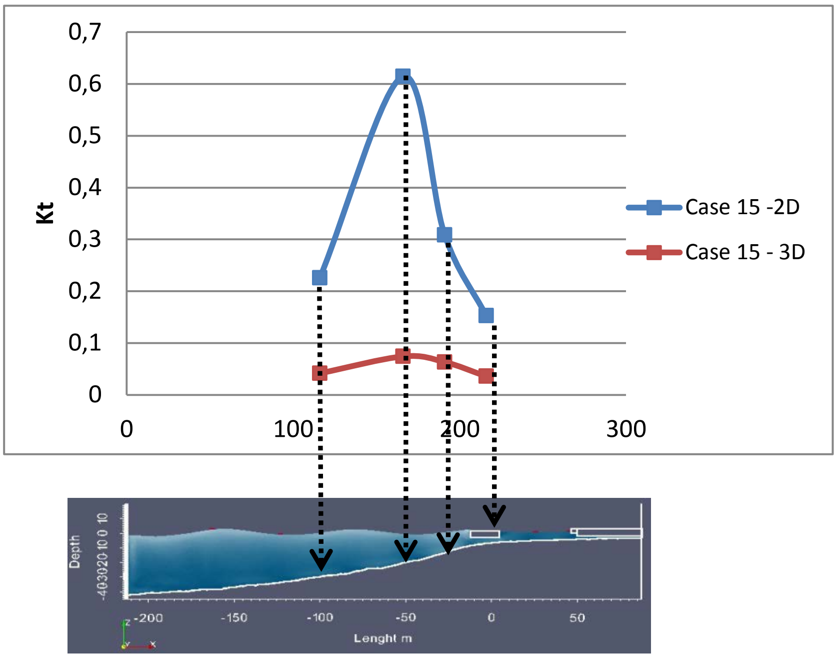

Figure 15. Case 15: FB Efficiency Comparison (2D vs. 3D)

5. CONCLUSIONS

- The SPH method is adequate to simulate with accuracy the interaction between water waves and a coastal protection structure, including the effect of an irregular bathymetry.
- However, physical phenomena, such as wave reflection, generated in 2D numerical wave tanks, are non realistic and must be carefully considered. Nevertheless, results derived with 2D models permits to assess efficiency of different structures with a low computational cost.
- The efficiency, in terms of the transmission coefficient, of the floating breakwater structure selected for the study case, evaluated under almost real conditions, for incident waves of 7s, is considerable high.
- It is shown that a structure with an area of 39 m^2, or with a volume of 1560 m^3, can protect adequately the pier with low environmental impacts.
- The proposed structure for the EGSAM pier reveals considerable advantages in contrast with conventional coastal protection structures, which must be evaluated in a wave channel, as part of the design process.

6. REFERENCES

1. Adee, B., Floating Breakwater Performance. Coastal Engineering, 15, pp.2777-2791, 1976.
2. Allyn, N., Watchorn, ernie., Jamieson, W., and Yang, G., Port of Brownsville Floating Breakwater. Proc. Ports Conference, 2001.
3. Batchelor, G., Introduction to Fluid Dynamics. Cambridge University Press, 1974.
4. Brebner, A., and Ofuya, A. Floating Breakwaters, Proceeding of 11th Conference on Coastal Engineering, London, 1968, ASCE, 2, pp. 1055-1094, 1969.
5. Bruce, L., Floating Breakwater Design, J. Waterway, Port, Coastal, Ocean Eng. 111, pp. 304-318, 1985.
6. Carr, J. H., Mobile Breakwater Studies: Hydrodynamics. Laboratory Report No. N-64.2, California Institute of Technology, 1950.
7. Centro de Investigaciones Oceanográficos e Hidrográficos. Climatología de los Principales Puertos del caribe Colombiano. 2010.
8. Chen, k., Wiegel, R.L., Floating breakwater for reservoir marines. Proc. Of the 12th Coastal Engineer. Pp. 487-506, 1970.
9. Crespo, A.J.C., Gómez-Gesteira, M. and Dalrymple, R.A., 3D SPH simulation of large waves mitigation with a dike. Journal of Hydraulic Research, 45(5), pp. 631- 642, 2007a.
10. Crespo, A.J.C., Gómez-Gesteira, M., Dalrymple, R.A., Modeling Dam Break Behavior over a Wet Bed by a SPH Technique. Journal of Waterway, Port, Coastal, and Ocean Engineering, 134(6), pp. 313-320, 2008.
11. Dalrymple, R. A., Rogers, B., Numerical modeling of water waves with the SPH method. Coastal Engineering, 53, pp. 141-147, 2006.
12. De la Sala, P., Revista de obras públicas. Rompeolas Flotantes. Vol. 14; pp. 165-167 and Vol.15, pp.178-181. 1873.
13. Fousert, M., Floating Breakwater: Theorical Study of a Dynamic wave Attenuating System. Master Thesis, Delft University of Technology, 2006.
14. Elchahal, G., Lafon, P., and Younes, R., Design Optimization of Floating Breakwaters with an interdisciplinary Fluid-Solid Structural Problem. Can. J. Civ. Eng., 36, pp. 1732-1743, 2009.
15. Gingold, R., and Monaghan, J., Smoothed Particle Hydrodynamics: Theory and Application to Non-Spherical Stars. Mon Not R Astr Soc, 181, pp. 375-389, 1977.
16. Gómez-Gesteira, M., Dalrymple, R.A., Using a three-dimensional smoothed particle hydrodynamics method for wave impact on a tall structure, Journal of. Waterway, Port, Coastal and Ocean Engineering, 130(2), pp. 63–69, 2004.
17. Gómez-Gesteira, M., D, Cerqueiro., A, Crespo., and R, Dalrymple., Green water overtopping analyzed with a SPH model. Ocean Engineering, 32, pp. 223-238, 2005.
18. Hales, Z.L., Floating Breakwaters: State of the Art, U.S Army Corps of Engineers. Technical Report No 81-1 Cap. 1. pp. 23-45, 1981.
19. He, F., Huang, Z., Wing, A., Hydrodynamic Perfonmance of a rectangular Floating Breakwater with and without Pneumatic Chambers: An Experimental Study. Ocean Engineering, 51, pp. 16-27, 2012.
20. Isaacson, M., and Sinha, s., Directional Wave effects on Large Offshore Structures. Journal of. Waterway, Port, Coastal and Ocean Engineering. 112 (4), pp. 482-497, 1986.
21. Isaacson, M., and Nwogu, OU., Wave Loads and Motions of Long Structures in Directional Seas. Journal of Offshore Mechanics and arctic Engineering, 109, pp. 126-132, 1987.
22. Jones, D., Transportable Breakwaters—A Survey of Concepts, Technical Report R-727, U.S. Navy Civil Engineering Laboratory, 1971.
23. Koutandos, E., Karambas, Th., Koutitas, C., Prinos, P., Floating Breakwaters Efficiency in Intermediate and Shallow Waters. Procceding of the 5th International Conference on Hydro –Science and Engineering, Portland, pp. 1-10, 2002.
24. Koutandos, E., Prinos, P., Gironella, X., Floating Breakwaters under Regular and Irregular Wave Forcing: Reflection and Transmission Characteristics. Journal of Hydraulic Research, 43(2), pp. 174-188, 2005.
25. Lucy, l., A numerical Approach to the testing of the Fission Hypothesis. Astron. J, 82(12), pp. 1013-1024, 1977.
26. Lo, E., And Shao, S., Simulations of Near-Shore solitary Wave Mechanics by an incompressible SPH Method. Applied Ocean research, 24, pp. 275-286.
27. Loukogeorgaki, E., Michailides, C., and Angelides, C., Hydroelastic Analysis of a Flexible Mat-Shaped Floating Breakwater under Oblique wave Action. Journal of Fluids and structures. 31, pp. 103-124, 2012.
28. Manuel, B., Response of a Pile restrained Floating Breakwater. Master Thesis, University of British Columbia, 1997.
29. Martinelli, L., Piero, R., Zanuttigh, B., Wave basin experiments on floating breakwaters with different layouts. Applied Ocean research, 30, pp. 199-207, 2008.

30. Monaghan, J., Smoothed Particle Hydrodynamics. Annual Rev Astron. Appl., 30, pp. 543-574, 1992.
31. Monaghan, J., Simulating free Surface Flows with SPH. Journal Computational Physics, 110, pp. 399-406, 1994.
32. Morris, J., and Kos, A., Solitary Waves on a Cretan Beach. Journal of Computational Physics, 136, pp. 214-226, 1997.
33. Murali, K., Amer, S. S., and Mani, J. S. Dynamics of cage floating breakwater. Journal of Offshore Mechanics and Arctic Engineering.Transactions of the ASME, 127(4), pp. 331-339, 1997.
34. Najafi, A., and Mazyak, A., Numerical Investigation of Floating Breakwater Movement using SPH Method. Inter J Nav Oc Engng, 3, pp. 122-125, 2011.
35. Peña, E., Ferreras, J., and Sanchez-Tembleque, F., Experimental study on wave transmission coefficient, mooring lines and module connector forces with different designs of floating breakwaters. Ocean Engineering, 38, pp.1150–1160, 2011.
36. Permanent International Association of navigation Congress – PIANC, Floating Breakwaters: A Practical Guide for Design and Construction. Report of working group No 13 of the permanent technical committee II, 1994.
37. Ramos, L., Vidal, L., Vilardy, S., Saavedra. L., Analysis of The Microbiological Contamination (Total And Fecales Coliforms) In The Bay Of Santa Marta, Colombian Caribbean. Acta biol. Colombiana, Vol. 13 (3) pp. 87 - 98, 2008.
38. Rabinovich, A., Long Ocean Gravity waves: Trapping, Resonance, and Leaking. Gidrometeoizzdat, (in Russian), pp. 325, 1993.
39. Richey, E.P., and Nece, R.E. , "Floating Breakwaters: State-of-the-Art," Proceedings of the Floating Breakwaters Conference, University of Rhode Island, Kingston, R.I., pp. 1-20. (1974).
40. Sannasiraj, SA., Sundar, V., Sundaravadivelu, R., Mooring Forces and Motion Responses of Pontoon-Type Floating breakwaters. Ocean Engineering, 25(1), pp. 27-48, 1998.
41. Sannasiraj, SA., Sundaravadivelu, R., Sundar, V., Difraction-radiation of Multiple Floating Structures in Directional Waves. Ocean Engineering, 28(2), pp. 201-234, 2000.
42. Shao, S., SPH simulation of a solitary wave interaction with a curtain-type breakwater. Journal of Hydraulic research, 43 (4), pp. 366-375, 2005.
43. Sorensen, R., Basic Wave Mechanics: for Coastal and ocean Engineers. John Wiley & Sons, inc. pp.241, 1993.
44. Stiassnie, M., A simple mathematical model of a floating breakwater, Applied Ocean Research, 2 (3), pp. 107-111, 1980.
45. Tadayon, N., Effect of geometric dimensions on the transmission coefficient of floating breakwaters. International Journal of Civil and Structural Engineering, 1(3), pp. 775-781, 2010.
46. Torum, A., Stansberg, C.T., Otterá, G.O., Sláttelid, O.H., Model tests on the CERC full scales test floating breakwater, final report, AD-A204 145. United States Army. 1987.
47. United State. U.S Army Corps of Engineers. Coastal Engineering Manual. EM 1110-2-1100, 3, pp. 1-36. 2002.
48. Volker, W., Floating Breakwater Performance Comparison. Coastal Engineering Proceedings, 17, pp. 2137-2158. 1980.
49. Wang, H., and Sun, Z., Experimental Study of a Porous Floating Breakwater. Ocean Engineering, 37, pp. 520-527, 2010.
50. Wehausen, J., Motion of Floating Bodies. Annual Review Of Fluid Mechanics, 3, pp. 237, 1971.
51. Williams A.N., and Abul-Azm A.G., Dual pontoon floating breakwater. Ocean Engineering. 24(5), pp. 465–78, 1997.
52. Williams, A., N., Lee, H.S., and Huang, Z., Floating pontoon breakwaters. Ocean Engineering. 27, pp. 221–240, 2000.
53. Yamamoto, T., Moored Floating Breakwater response to regular and Irregular Waves. Applied Ocean Research, 3, pp. 85-92, 1981
54. Yoon, J., and Cho, S., Experimental Research on Effective Floating Breakwaters. Journal of Coastal Research, Special Issue 64, pp. 631 – 635, 2011.